Available online at www.sciencedirect.com
ScienceDirect
Catalysis Today 116 (2006) 498–504
CATALYSIS TODAY
www.elsevier.com/locate/cattod

Effect of solvo-thermal treatment temperature on the properties of sol–gel ZrO_2–TiO_2 mixed oxides as HDS catalyst supports

María C. Barrera [a], José Escobar [b,*], José A. de los Reyes [a], María A. Cortés [b], Margarita Viniegra [a], A. Hernández [c]

[a] *Universidad Autónoma Metropolitana-Iztapalapa, San Rafael Atlixco 186, Col. Vicentina, Iztapalapa, 09340 México, D.F., Mexico*
[b] *Instituto Mexicano del Petróleo, Eje Central Lázaro Cárdenas 152, San Bartolo Atepehuacan, G.A. Madero, 07730 México, D.F., Mexico*
[c] *Universidad Autonóma Metropolitana-Azcapotzalco, San Pablo 180, Reynosa, Tamaulipas, Azcapotzalco, D.F., 02200 México, Mexico*

Available online 18 July 2006

Abstract

ZrO_2–TiO_2 mixed oxide (30–70 mol/mol) was prepared by low-temperature sol–gel followed by solvo-thermal treatment (1 day) at various temperatures (40, 80, 120, 160 and 200 °C). Selected samples of the corresponding single oxides were also prepared. Materials characterization was carried out by N_2 physisorption, XRD, thermal analysis (TG-DTA) and UV–vis DRS, infra-red and Laser-Raman spectroscopies. Binary solids of enhanced pore volume and pore size diameter were obtained by increasing the post-treatment severity. Anatase TiO_2 micro-segregation was evidenced by Raman spectroscopy for the mixed oxide solvo-treated at the highest temperature. This solid also showed the highest crystallization temperature to $ZrTiO_4$ (~702 °C). Mo impregnated (2.8 atom nm^{-2}) on various mixed oxides was sulfided under H_2S/H_2 (400 °C, 1 h), the catalysts being tested in the dibenzothiophene hydrodesulfurization (HDS, T = 320 °C, P = 5.59 MPa). By increasing the severity of the solvo-treatment improved supports for MoS_2 phase were obtained. The HDS activity of the catalyst with carrier post-treated at 200 °C was ~40% higher (in per total mass basis) than that of sulfided Mo supported on the binary oxide solvo-treated at 80 °C. The ZrO_2–TiO_2-supported catalysts showed higher selectivity to products from the hydrogenation route than their counterparts supported on either single oxide.

Keywords: Zirconia–Titania; Sol–gel; Solvo-thermal treatment; Dibenzothiophene hydrodesulfurization; Raman spectroscopy

1. Introduction

Ever stricter environmental regulations on S content in oil-derived distillates demand improved hydrodesulfurization (HDS) catalysts. In this context, ZrO_2–TiO_2 mixed oxides have recently attracted attention as hydrotreating (HDT) catalyst supports [1,2]. Those binary systems have shown very promising properties as catalyst themselves when applied in numerous reactions, as recently presented in a review by Reddy and Khan [3]. To overcome the low porosity and reduced pore diameter that have been commonly reported for zirconia–titania formulations, different synthesis methodologies have been applied [4–7]. Recently, we reported that solvo-thermal post-treatment of precursors prepared by sol–gel resulted in wide-pore ZrO_2–TiO_2 (30–70 mol/mol) [8].

Solvo-thermal methods have attracted attention in the preparation of various mixed oxides (ZrO_2–Al_2O_3 [9], Al_2O_3–TiO_2 [10], Eu_2O_3–TiO_2 [11]) from metal alkoxide precursors, providing materials of improved textural and surface properties.

In our previous work [8], we found that solvo-treatment temperature (STT) of 80 °C (under autogenic pressure, per 1 day) resulted in materials of high surface area (S_g ~338 m^2 g^{-1}), high pore volume (V_p ~0.98 cm^3 g^{-1}) and wide pores (~8.9 nm). However, in that investigation we just tried two very different temperatures (80 and 240 °C) making difficult to reach conclusions about the optimal value of that parameter. After treatment at very severe conditions (240 °C) the mixed matrices retained very poor texture due to phase segregation (to monoclinic ZrO_2 and anatase TiO_2). Surface acidity of the samples was also affected by temperature and duration of solvo-treatments [8]. Although we found further improvements on the properties of the mixed oxides as HDS catalyst supports (probably due to increased Lewis acid sites strength) by increasing duration of solvo-treating from 1 to 4 days, we considered that the magnitude of that

* Corresponding author. Tel.: +52 55 9175 8389; fax: +52 55 9175 6380.
E-mail address: jeaguila@imp.mx (J. Escobar).

0920-5861/$ – see front matter
doi:10.1016/j.cattod.2006.06.030

effect (about 21% increased activity, in pseudo kinetic constant basis) did not justify to use long post-treatments that could add complexity to the synthesis method.

In this work, we undertook a study on the effect of temperature of solvo-thermal treatment (in the 40–200 °C range) on physicochemical properties of ZrO_2–TiO_2 at 30–70 mol/mol, as it is known that surface area is maximized at this composition [12]. Samples of the corresponding single oxides prepared at selected STT were also studied. Materials were characterized by N_2 physisorption, XRD, thermal analysis and UV–vis DRS, infra-red and Laser-Raman spectroscopies. This technique was also applied to study the impregnated Mo phase. To evaluate the influence of improved textural properties on HDS activity of ZrO_2–TiO_2-supported MoS_2 catalysts, binary oxides were impregnated at 2.8 Mo atoms nm^{-2} by incipient wetness and tested in the liquid phase dibenzothiophene hydrodesulfurization.

2. Experimental

2.1. Materials synthesis

ZrO_2–TiO_2 (ZT, 30–70 mol/mol) was synthesized by low-temperature sol–gel method followed by solvo-thermal treatment [8]. Zr(IV) propoxide and Ti(IV) isopropoxide (both from Aldrich) were diluted in isopropanol (ROH, Baker). A de-ionized H_2O + HNO_3 (Baker) mixture was drop-wise added to the alkoxides solution kept under vigorous stirring at ∼0 °C. The ROH/alkoxides, H_2O/alkoxides and HNO_3/alkoxides mol ratios used were 65, 20 and 0.05, respectively. After alkoxide hydrolysis, the resulting alcogels submerged in the mother liquor were brought to a stainless steel hermetic autoclave (Parr 4560) and treated at different solvo-treatment temperature STT (40, 80, 120, 160 and 200 °C) per 1 day under autogenic pressure. Then, materials were vacuum-dried until total solvent elimination, treated at 120 °C (2 h) and finally calcined at 500 °C (4 h) under static air atmosphere. Some samples of ZrO_2 (Z) and TiO_2 (T) single oxides were prepared through similar protocols, including solvo-treatment at either 80 or 200 °C.

Selected supports calcined at 500 °C were impregnated at incipient wetness with $(NH_4)_6Mo_7O_{24}{\cdot}4H_2O$ (Aldrich) at 2.8 Mo atoms nm^{-2}. The impregnated materials were dried at 120 °C (2 h) after aging at room temperature (overnight). The final catalysts were obtained by sulfiding at 400 °C (1 h) under a H_2S/H_2 stream (Praxair, 15/85% vol./vol., 4 L h^{-1}). The dried impregnated precursors were brought to the sulfiding temperature (at 10 °C min^{-1}) under N_2 flow (4 L h^{-1}). Once the required conditions were attained, the inert gas flow was switched to the H_2S/H_2 mixture.

2.2. Materials characterization

N_2 physisorption at −196 °C (Autosorb Quantachrome) was used for textural characterization. By repeated determinations, experimental error amounting to less than 5% of the reported values of surface area and pore volume was evidenced. Structural order was studied by X-ray diffraction (Siemens D-500 Kristalloflex, Cu Kα radiation, λ = 0.15406 nm). Thermal analyses were carried out with a Netzch Thermische Analyze, STA 409 EP apparatus under static air atmosphere. UV–vis absorption spectra (in powders) were obtained by an Ocean Optics USB2000 miniature optic fiber spectrometer. Wafers (∼1.3 cm of diameter) constituted by samples to be studied diluted with KBr (J.T. Baker Inc., IR grade) were analyzed at room temperature with a FT-IR apparatus Perkin-Elmer Spectrum One (50 scans at 4 cm^{-1} resolution). Raman spectra of supports and impregnated materials were measured at room temperature using a Jobin Yvon Inc. Horiba T64000 spectrometer, equipped with a confocal microscope (Olympus, BX41) with the 514.5 nm line from Ar^+ laser (5 mW).

2.3. DBT HDS reaction test

Sulfided catalysts were tested in dibenzothiophene (DBT, Aldrich) HDS in a slurry batch reactor (Parr 4562 M), using *n*-hexadecane (Aldrich) as solvent. The reaction mixture was prepared by dissolving ∼0.3 g of DBT in 100 cm^3 of *n*-hexadecane (98 mass% and 99 + mass%, respectively; both from Aldrich) and adding ∼0.2 g of sieved catalyst (80–100 Tyler mesh, 0.165 mm average particle diameter). Operating conditions (carefully chosen to avoid external and internal diffusional limitations) were $P = 5.59 \pm 0.03$ MPa, $T = 320 \pm 2$ °C and 1000 rpm (∼105 rad s^{-1}) mixing speed. Samples taken periodically were analyzed in a gas chromatograph Perkin-Elmer AutoSystem XL (flame ionization detector and Econo-Cap-5 capillary column from Alltech). HDS kinetic constants were calculated assuming pseudo-first-order kinetics referred to DBT concentration (x = conversion, t = time):

$$k = \frac{-\ln(1-x)}{t} \quad (1)$$

k_{DBT} values were normalized by considering reaction volume and mass of catalyst used (k_{DBT} in $m^3\,kg_{cat}^{-1}\,s^{-1}$). By repeated HDS activity experiments it was found that the error implied in the determined values of pseudo kinetic constant was less than 5%.

3. Results and discussion

3.1. Supports characterization

From Table 1, by increasing the STT just slight changes in surface area of ZrO_2–TiO_2 oxides were observed. These surface area values were notably larger than that reported for zirconia–titania oxides of similar composition prepared by co-precipitation in basic media [13]. On the other hand, pore volume progressively increased with STT. Excepting ZT40 and ZT80, for the rest of binary samples pore volume was superior as compared with previously reported values [4,6]. The sample submitted to the highest STT (ZT200) had the maximum in both pore volume and pore size. From Fig. 1 where pore size distributions (PSD) calculated from the adsorption branch of the corresponding N_2 adsorption isotherms are shown, all the binary oxides showed pore size much higher than those

Table 1
Textural properties of ZrO_2–TiO_2 mixed oxides (30–70 nominal formulation) prepared at various solvo-thermal treatment temperatures

Sample	STT (°C)	S_g ($m^2\ g^{-1}$)	V_p ($cm^3\ g^{-1}$)
ZT40	40	287	0.43
Z80	80	75	0.62
T80	80	101	0.26
ZT80	80	292	0.57
ZT120	120	304	0.74
ZT160	160	304	0.76
Z200	200	99	0.73
T200	200	129	0.64
ZT200	200	324	0.96

Materials calcined at 500 °C.

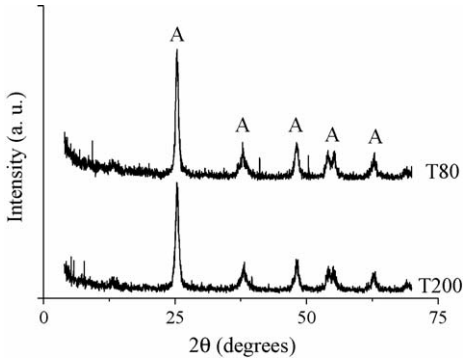

Fig. 2. X-ray diffractograms of sol–gel TiO_2 solvo-treated at either 80 or 200 °C. Samples calcined at 500 °C. A: TiO_2 anatase.

commonly reported for this kind of materials, when prepared by either co-precipitation [14] or sol gel [15]. The wide PSD profiles suggested that solid particles of different sizes constituted the mixed solid matrices. The materials could be divided in medium-pore and large-pore oxides, the ZT40 and ZT80 belonging to the former group meanwhile the rest of samples could be classified in the latter. The pore size of these materials (∼9–12 nm) was larger than those in the range considered optimum for catalysts to be applied in the HDT of middle distillates [16]. Poly-condensation reactions of partially hydrolyzed zirconium and/or titanium species could continue during solvo-treatment at different temperatures. Thus, the extent of removal of non-hydrolyzed alkoxy groups still attached to Zr^{4+} or Ti^{4+} cations could depend on the severity of the treatment. That organic residua elimination could promote M–O–M linkages formation (M = Zr^{4+} or Ti^{4+}) then contributing to particle growth. The last could also take place by dissolution and re-precipitation process (coarsening, ripening, etc.) [17]. This phenomena could result in inter-particle spaces (pores) which size could be directly related to post-treatment conditions. Very recently, Liu et al. [11] have also reported high surface area, high porosity and wide pores (∼11.2 nm) in Eu_2O_3–TiO_2 solids prepared by using a solvo-thermal method at 120 °C, although in this case they additionally used an organic pore-directing agent.

The textural properties of ZrO_2 and TiO_2 single oxides were also influenced by STT (Table 1), that effect being clearer for the latter. Notably, the surface area and pore volume of T200 were similar to those of the high-surface area titania manufactured by Chiyoda [18] but with pore size even larger.

By X-ray diffraction, all the mixed oxides calcined at 500 °C were amorphous (not shown) indicating strong interaction between components as no definite phases of zirconia or titania were identified [7,13]. As reported in our previous paper [8], after solvo-treatment at very severe conditions (240 °C), well-defined separated domains of monoclinic ZrO_2 and anatase TiO_2 could be identified. According to our new data, that phase segregation could start during solvo-treatment at temperatures higher than 200 °C, as this phenomenon was not observed in the ZT200 sample. For the single oxides solvo-treated at different conditions no important differences in structural order were observed, where titania crystallized to anatase (Fig. 2) while zirconia (Fig. 3) was composed of a mixture of monoclinic and tetragonal phases. The proportion of the latter was lower for the Z200 oxide. Regarding titania samples, the pore size distribution of T200 (not shown) included much wider pores to those of T80 suggesting larger particle size for the former. Considering that the crystal size of T200 was smaller to that of T80 (Fig. 2), it seemed that the latter was constituted by agglomerates of lower number of crystals.

By thermogravimetrical analyses, no very important differences in weight loss (in the 100–450 °C range) among samples of as-synthesized (non-calcined) binary oxides were registered (Table 2). However, it seemed that the samples solvo-

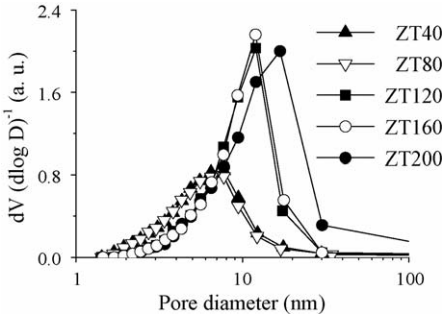

Fig. 1. Effect of solvo-thermal treatment temperature on pores size distribution of sol–gel ZrO_2–TiO_2 (30–70 nominal molar formulation) samples calcined at 500 °C.

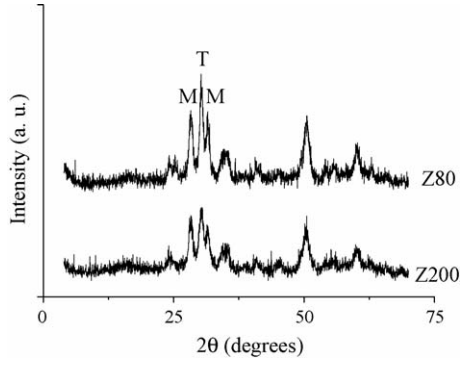

Fig. 3. X-ray diffractograms of sol–gel ZrO_2 solvo-treated at either 80 or 200 °C. Samples calcined at 500 °C. M: monoclinic; T: tetragonal.

Table 2
Weight losses in the 120–450 °C range (as determined by thermogravimetrical analysis) and $ZrTiO_4$ crystallization temperature (as determined by DTA) in ZrO_2–TiO_2 mixed oxides (30–70 nominal formulation) prepared at various solvo-thermal treatment temperatures

Support	Weight loss (%)	$ZrTiO_4$ crystallization temperature (°C)
ZT40	23	684
ZT80	21	695
ZT120	19	697
ZT160	20	694
ZT200	18	702

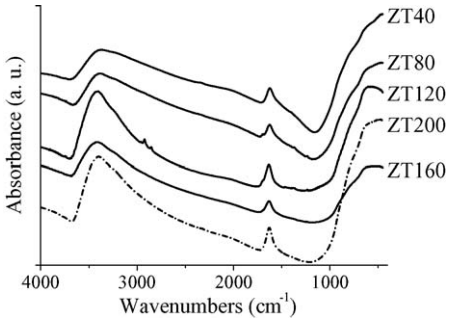

Fig. 5. Infrared spectra of sol–gel ZrO_2–TiO_2 (30–70 nominal molar formulation) prepared at various solvo-thermal treatment temperatures. Samples calcined at 500 °C.

treated at lower temperatures retained slightly higher amounts of organic residua suggesting that condensation reactions could be more complete in solids prepared at more severe STT. The differential thermal analyses (DTA) profiles of binary oxides (not shown) were similar to that previously found for the ZT80 oxide [8]. The exothermal inflection related to crystallization to $ZrTiO_4$ [19] slightly shifted to higher temperature with the severity of solvo-treatment (Table 2). Andrianainarivelo et al. [19] observed similar phenomena for equimolar ZrO_2–TiO_2 samples prepared from different precursors by using a non-hydrolytic sol–gel route, these variations in crystallization temperature being considered function of the homogeneity of the studied samples. Thus, the increase in that parameter with the STT could reflect progressive phase segregation in the binary oxides prepared at the more severe conditions. However, this effect could take place at a micro-scale level, as it could not be detected by XRD (not shown). In all our binary samples ZrO_2–TiO_2 (30–70) titania excess seemed to be well-dissolved in the $ZrTiO_4$ matrix as exothermal peaks due to crystallization to any TiO_2 phase were absent suggesting impeded crystal growth.

UV–vis DRS spectra of supports calcined at 500 °C are shown in Fig. 4. In all cases, the mixed oxides had bands registered at intermediate wavelength values as to those corresponding to ZrO_2 and TiO_2 single oxides (204–209 and 350–360 nm range, respectively [8]) indicating strong interaction between components [20]. Although no very significant

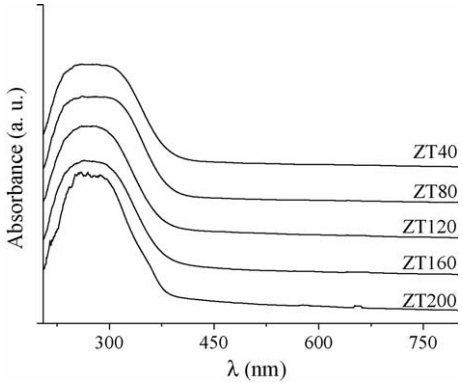

Fig. 4. UV–vis DRS spectra of sol–gel ZrO_2–TiO_2 (30–70 nominal molar formulation) prepared at various solvo-thermal treatment temperatures. Samples calcined at 500 °C.

differences in absorption edge position were observed, it appeared that by raising STT in the 40–160 °C range integration of the components was improved, as slight shifts to higher energies suggested increased insulating character in the binary solids by ZrO_2 influence. However, it appeared to be an optimum STT value to obtain highly homogeneous matrices as the absorption edge of the binary oxide prepared at the more severe conditions (ZT200) red-shifted as to that of ZT120 and ZT160 °C perhaps indicating micro-scale titania segregation.

Infrared spectra for various mixed oxides are shown in Fig. 5. The band observed at ~3450 cm^{-1} that could be attributed to molecular water which covers the terminal OH groups [21]) was more intense for samples synthesized at high STT. As no bands related to the frequencies of bridging or multi-centered OH groups could be detected it could be concluded that all surface hydroxyls present on the mixed oxides were terminal, in agreement with that reported by Zou and Lin [21]. Although the more intense bands found for ZT120, ZT160 and ZT200 could be partially due to the higher surface area of these samples, they suggested variations in surface composition as to that of the samples prepared at milder conditions (ZT40 and ZT80). Changes in surface composition could be induced by solvo-thermal conditions. Indeed, solvo-treating at 80 °C resulted in surface zirconia enrichment for ZrO_2–TiO_2 (30–70) mixed oxides, where a nearly equimolar surface composition was registered (by XPS) [8]. The slight blue-shift of the bands related to OH groups on ZT120 and ZT160 (3415 and 3417 cm^{-1}, respectively) as to those of ZT40, ZT80 and ZT200 (3377, 3392 and 3395 cm^{-1}, respectively) could indicate their higher basicity [22]. This property could influence the magnitude of the interaction with the supported Mo phase as it is well-known that molybdate anions preferably interact with this kind of sites [23]. Band at ~1625 cm^{-1}, which was more intense for ZT200, could be attributed to un-dissociated water molecules coordinated to surface cationic centers [24]. Again, those corresponding to ZT120 and ZT160 (at 1633 and 1630 cm^{-1}, respectively) slightly blue-shifted as to those of ZT40, ZT80 and ZT200 (1621, 1622 and 1626 cm^{-1}, respectively) suggesting stronger interaction between adsorbed water and surface cationic species in the mixed oxides where, as aforementioned, the components seemed to be in higher interaction. Finally, the absorptions in the 750–450 cm^{-1} range with contributions from monoclinic and tetragonal ZrO_2 and anatase TiO_2 [25], were more defined for

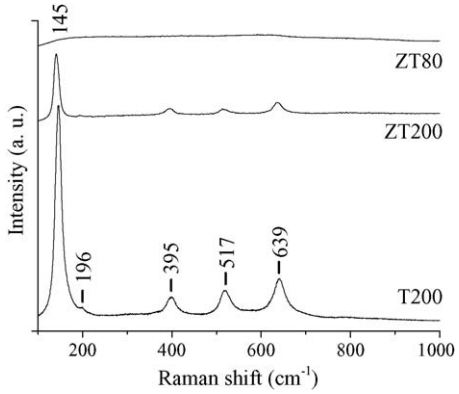

Fig. 6. Raman spectra of sol–gel ZrO_2–TiO_2 (30–70 nominal molar formulation) solvo-treated at either 80 or 200 °C. That of the TiO_2 sample solvo-treated at 200 °C included for sake of comparison. Samples calcined at 500 °C.

solids prepared at higher STT again suggesting some degree of micro-segregation.

Raman spectrum of the T200 support showed six Raman actives modes (located at 145, 196, 395, 517, 639 and 700 cm^{-1}) assigned to anatase TiO_2 structure ($A_{1g} + 2B_{1g} + 3E_g$ [26]; Fig. 6). When the support was composed by zirconia and titania (ZT200) the corresponding Raman spectrum showed the same bands attributed to anatase phase but with significantly lower intensity. Any vibrating bands corresponding to zirconia phase were not registered. The observed bands suggested that some micro-crystallites of anatase could be present in ZT200, although their size must be less than 3 nm, as they remained undetected by XRD (not shown). For the rest of zirconia–titania mixed oxides solvo-treated at lower temperatures no bands were observed in the corresponding Raman spectra, indicating that they were completely amorphous (see, for instance, ZT80 spectrum in Fig. 6).

3.2. Impregnated precursors characterization

Raman spectra of dried Mo impregnated precursors are shown in Fig. 7. Additionally to the vibrations bands observed from the supports (Fig. 6), a broad band in 944 cm^{-1} which could be assigned to hydrated polymeric molybdenum oxide species in octahedral environment [27] was registered for Mo/ZT200. The Raman spectrum of MoT200 showed a weak band at 796 cm^{-1} due to the first overtone of the signal at ~395 cm^{-1} band of anatase TiO_2 [28]. The Mo/ZT80 just showed the vibrating band corresponding to polymeric surface molybdate, as the support was completely amorphous (Fig. 6). The ammonium heptamolybdate impregnating solutions at their acidic natural pH contained just octahedral species [29] that could originate the hydrated poly-molybdates identified on the surface of the supports. The Raman spectra of various impregnated precursors did not show any indication of polycrystalline MoO_3 (bands at 820 and 996 cm^{-1} [18]) suggesting high dispersion of supported molybdenum on all the studied oxides. The high pore volume of solvo-treated supports (Table 1) could contribute to this fact, as this characteristic precluded utilization of highly concentrated impregnating solutions.

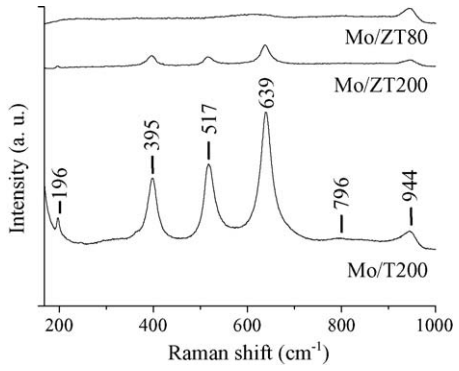

Fig. 7. Raman spectra of Mo impregnated (2.8 atom nm^{-2}) on sol–gel ZrO_2–TiO_2 (30–70 nominal molar formulation) solvo-treated at either 80 or 200 °C. Mo impregnated at the same concentration on TiO_2 sample solvo-treated at 200 °C also included. Impregnated precursors dried at 120 °C.

3.3. DBT HDS activity test

As could be seen from Table 3, the sulfided Mo catalysts (2.8 atom nm^{-2}) supported on a sol–gel ZrO_2–TiO_2 of similar composition as to that of the mixed oxides presently studied but not solvo-thermally treated had much lower activity in dibenzothiophene hydrodesulfurization evidencing the benefits obtained from those post-treatments. Because of their higher surface area (Table 1) that enabled to increase the loading of well-dispersed Mo (Fig. 7), the solvo-treated mixed oxides favored obtaining sulfided catalysts much more active than their counterparts supported on either single oxide. The HDS activity found over sulfided Mo/ZT200 catalyst was especially remarkable.

Taking into account the differences in surface area of the supports (then in Mo loading) the intrinsic HDS reaction rate could be a better basis of comparison (Fig. 8). Similarly to that previously observed for MoS_2 supported on non-solvo-treated sol–gel oxides [30] where the intrinsic activity in DBT HDS (at similar operating conditions than in the present case) of the sulfided catalysts with ZrO_2–TiO_2 carrier was lower as to that of

Table 3
Pseudo-first-order kinetic constants (DBT HDS) promoted by various MoS_2 catalysts supported on sol–gel ZrO_2, TiO_2 or ZrO_2–TiO_2 (30–70 nominal molar formulation) solvo-treated at either 80 or 200 °C and calcined at 500 °C

Sample	Mo (wt%)	k ($\times 10^{-6}$ m^3 kg_{cat}^{-1} s^{-1})
Mo/ZT[a]	11.45	2.47
Mo/Z80	3.24	1.97
Mo/T80	4.31	3.05
Mo/ZT80	11.52	6.45
Mo/Z200	4.23	3.24
Mo/T200	5.4	3.41
Mo/ZT200	12.62	9.05

$P = 5.59 \pm 0.03$ MPa, $T = 320$ °C, 1000 rpm (~105 rad s^{-1}) mixing speed, solvent: *n*-hexadecane.

[a] With sol–gel ZrO_2–TiO_2 (30–70) support non-solvothermally treated (from Ref. [8]).

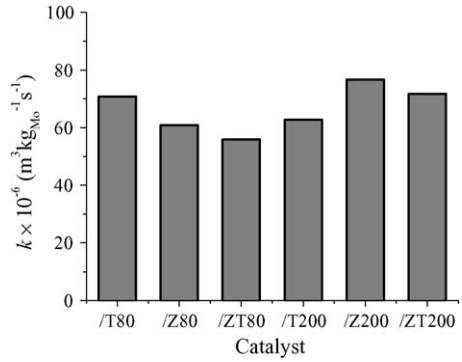

Fig. 8. Pseudo-first-order intrinsic kinetic constants (DBT HDS) promoted by sulfided Mo (2.8 atom nm^{-2}) supported on ZrO_2, TiO_2 or ZrO_2–TiO_2 (30–70 nominal molar formulation) solvo-treated at either 80 or 200 °C and calcined at 500 °C. $P = 5.59 \pm 0.03$ MPa, $T = 320 \pm 2$ °C, 1000 rpm (∼105 rad s^{-1}) mixing speed, solvent: *n*-hexadecane.

Mo/TiO_2, Mo supported on T80 was more efficient in hydrodesulfurization than when impregnated on the ZT80 oxide. However, the difference in intrinsic activity between the sulfided catalyst supported on the binary oxide and that with titania carrier was less pronounced than that previously reported [30]. Excepting Mo/T200, the catalysts supported on the oxides synthesized at more severe conditions showed higher intrinsic HDS activity than those with carrier post-treated at 80 °C. The hydrodesulfurizating properties of Mo/ZT200 were especially remarkable considering that its intrinsic activity was similar to that of the best formulation (Mo/Z200), with the additional advantage of having a carrier of much higher surface area (Table 1). This characteristic enabled to triple the Mo loading in the final catalyst (Table 3).

The DBT HDS selectivity pattern (at ∼10% conversion) found for the studied sulfided Mo catalyst is shown in Fig. 9. Although direct desulfurization (DDS [31]) to biphenyl (BP) was favored over all materials, the proportion BP/(HDBT'S + CHB) was different for catalyst supported on ZrO_2, TiO_2 or the mixed oxides. No bicyclohexyl formation from saturation of the remaining aromatic ring of cyclohexylbenzene was observed. Considering that BP hydrogenation to CHB could be strongly inhibited by DBT competitive

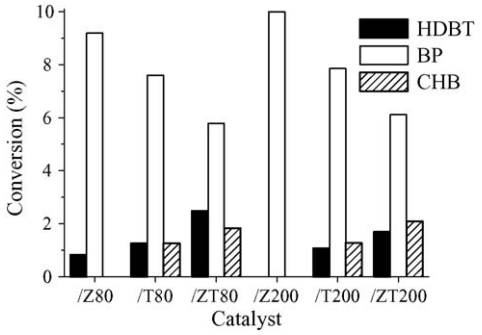

Fig. 9. Selectivity patterns (at ∼10% conversion, DBT HDS) promoted by sulfided Mo (2.8 atom nm^{-2}) supported on ZrO_2, TiO_2 or ZrO_2–TiO_2 (30–70 nominal molar formulation) solvo-treated at either 80 or 200 °C and calcined at 500 °C. $P = 5.59 \pm 0.03$ MPa, $T = 320 \pm 2$ °C, 1000 rpm (∼105 rad s^{-1}) mixing speed, solvent: *n*-hexadecane. BP: biphenyl; HDBT: hexahydro- + tetrahydro-DBT; CHB: cyclohexylbenzene; BCH: bicyclohexyl.

adsorption under our HDS conditions [32], we considered that all CHB came from HYD route [31]. Then, selectivity to DDS/selectivity to HYD could be expressed as the BP/(HDBT'S + CHB) ratio. As previously found [30], sulfided Mo supported on ZrO_2 strongly favored biphenyl formation. Even more, for Mo/Z200 BP was the only product observed. For TiO_2-supported catalysts we previosuly observed [30] approximately 50% selectivity oriented to biphenyl, being the rest hydrogenated products. In the present case, however, Mo/T80 and Mo/T200 had a stronger preference for DDS route suggesting that solvo-treatment could impart distinctive surface properties to titania, as to those of the non-solvo-treated sol–gel oxide. These properties could in turn modify other factors that exert direct influence on selectivity, namely, distribution of the primary dihydrointermediates, hydrogen availability on the catalytic centers on which they adsorb and basicity of the S anions associated to catalytic centers [33]. A clear improvement on the hydrogenating properties of the sulfided Mo phase originated by its interaction with the mixed oxides support could be observed (Fig. 9). Interestingly, solvo-treatment temperature did not seemed to appreciably affect the magnitude of that effect. Even more, those selectivity patterns observed were quite similar to that found for sulfided Mo catalyst (at 2.8 atom nm^{-2}) supported on non-solvo-treated sol–gel zirconia–titania mixed oxide of similar composition [8]. Catalysts of enhanced hydrogenating power are particularly interesting as aromatic ring saturation facilitates the desulfurization of sterically hindered organo-sulfur compounds [34] which removal results critical for the production of ultra-low sulfur oil-derived middle distillates. According to the ''rim-edge'' model proposed by Daage and Chianelli [35] changes in selectivity in the DBT HDS could indicate differences in stacking degree of MoS_2 supported particles, considering that crystallites composed of lower number of stacked layers could favor the hydrogenation route (HYD) over DDS. Deeper catalyst characterization (mainly focused in the sulfided active phase properties) is needed to shed light in the origin of the selectivity variations observed.

So far, it is not possible to attribute the enhanced HDS activity of MoS_2 catalysts supported on oxides solvo-treated at high temperature to any specific characteristic neither from the support nor from the active sulfided phase. Solvo-treated zirconia–titania sol–gel oxides (and the corresponding supported MoS_2 catalysts) deserve much more detailed studies because of their very promising properties as HDS catalyst supports.

4. Conclusions

Texture of ZrO_2–TiO_2 mixed oxides (30–70) prepared by low-temperature sol–gel was improved by increasing the severity of solvo-thermal treatment conditions. High surface area, high pore volume, wide-pore materials could be prepared by solvo-treating at 200 °C that provoked anatase TiO_2 micro-segregation, as evidenced by Raman spectroscopy. In all impregnated materials deposited Mo (at 2.8 atom nm^{-2}) was present as octahedral polymolybdates suggesting well-dispersed species, as no definite

MoO_3 domains were registered. Sulfided Mo catalyst of improved hydrodesulfurizating activity was obtained when supported on the mixed oxide solvo-treated at the more severe conditions. The observed increase in activity (in pseudo kinetic constant basis, dibenzothiophene hydrodesulfurization) was of about 40%, as compared to that over a similar catalyst impregnated on a binary oxide solvo-treated at milder conditions (80 °C). Even more, the HDS activity was improved by a factor of ∼3.7, as to that of a MoS_2 catalyst impregnated on non-solvo-treated sol–gel zirconia–titania of the same composition (of alike surface area but much lower porosity and pore size). The mixed oxides-supported catalysts showed higher selectivity to products from the hydrogenation route (hydrodibenzothiophenes and cyclohexylbenzene) than their counterparts supported on either single oxide.

Acknowledgements

The authors recognize financial support from Instituto Mexicano del Petróleo (FIES 98-117-II D.0090 grant), CONACYT (Project 42204) and UAM-Iztapalapa. María C. Barrera is also indebted to CONACYT for a graduate student scholarship (95326).

References

[1] S.K. Maity, M.S. Rana, S.K. Bej, J. Ancheyta, G. Murali Dhar, Catal. Lett. 72 (2001) 115.
[2] C.-M. Lu, Y.-M. Lin, I. Wang, Appl. Catal. A 198 (2000) 223.
[3] B.M. Reddy, A. Khan, Catal. Rev. 47 (2005) 257.
[4] F.P. Daly, H. Ando, J.L. Schmitt, E.A. Sturm, J. Catal. 108 (1987) 401.
[5] F.P. Daly, H. Ando, H.C. Foley, H.J. Jung, US Patent 5,021,385 (1991).
[6] F.P. Daly, J. Catal. 116 (1989) 600.
[7] J.G. Weissman, E.I. Ko, S. Kaytal, Appl. Catal. A 94 (1993) 45.
[8] M.C. Barrera, M. Viniegra, J. Escobar, M. Vrinat, J.A. De Los Reyes, F. Murrieta, J. García, Catal. Today 98 (2004) 131.
[9] O. Metelkina, N. Hüsing, P. Pongratz, U. Schubert, J. Non-Cryst. Solids 285 (2001) 64.
[10] M. Kang, Mater. Lett. 59 (2005) 3122.
[11] Zh. Liu, J. Zhang, B. Han, J. Du, T. Mu, Y. Wang, Zh. Sun, Micropor. Mesopor. Mater. 81 (2005) 169.
[12] C. Lahousse, A. Aboulayt, F. Maugé, J. Bachelier, J.C. Lavalley, J. Mol. Catal. 84 (1993) 283.
[13] V. Vishwanathan, H.-S. Roh, J.-W. Kim, K.-W. Jun, Catal. Lett. 96 (2004) 23.
[14] D. Mao, Q. Chen, G. Lu, Appl. Catal. A 244 (2003) 273.
[15] M.E. Manríquez, T. López, R. Gómez, J. Navarrete, J. Mol. Catal. A 220 (2004) 229.
[16] A.L. Dicks, R.L. Ensell, T.R. Phillips, A.K. Szczepura, M. Thorley, A. Williams, R.D. Wragg, J. Catal. 72 (1981) 266.
[17] C.J. Brinker, G.W. Scherer, Sol–Gel Science, Academic Press Inc., San Diego, CA, 1990, p. 360.
[18] S. Dzwigaj, C. Louis, M. Breysse, M. Cattenot, V. Belliere, C. Geantet, M. Vrinat, P. Blanchard, E. Payen, S. Inoue, H. Kudo, Y. Yoshimura, Appl. Catal. B 41 (2003) 181.
[19] M. Andrianainarivelo, R.J.P. Corriu, D. Leclercq, P.H. Mutin, A. Viouxs, J. Mater. Chem. 7 (1997) 279.
[20] H.-R. Chen, J.-L. Shin, J. Yu, L.-Z. Wang, D.-S. Yan, Micropor. Mesopor. Mater. 39 (2000) 171.
[21] H. Zou, Y.S. Lin, Appl. Catal. A 265 (2004) 35.
[22] Y. Yue, X. Zhao, W. Hua, Z. Gao, Appl. Catal. B 46 (2003) 561.
[23] N.Y. Topsøe, H. Topsøe, J. Catal. 139 (1993) 631.
[24] C. Morterra, J. Chem. Soc. Faraday Trans. 1 (84) (1988) 1617.
[25] M. Daturi, A. Cremona, F. Milella, G. Busca, E. Vogna, J. Eur. Ceram. Soc. 18 (1998) 1079.
[26] U. Balachandran, N.G. Eror, J. Solid State Chem. 42 (1982) 276.
[27] J. Miciukiewicz, T. Mang, H. Knözinger, Appl. Catal. A 122 (1995) 151.
[28] T.J. Dines, C.H. Rochester, A.M. Ward, J. Chem. Soc. Faraday Trans. 87 (1991) 643.
[29] G. Xiong, Zh. Feng, J. Li, Q. Yang, P. Ying, Q. Xin, C. Li, J. Phys. Chem. B 104 (2000) 3581.
[30] M.C. Barrera, J. Escobar, C. Marín, M. Viniegra, J.A. De Los Reyes, J.G. Pacheco, F. Murrieta, Pet. Sci. Technol. 22 (2004) 87.
[31] M. Houalla, N. Nag, A.V. Sapre, D.H. Broderick, B.C. Gates, AIChE J. 24 (1978) 1015.
[32] E.J.M. Hensen, P.J. Kooyman, Y. van der Meer, A.M. van der Kraan, V.H.J. de Beer, J.A.R. van Veen, R.A. van Santen, J. Catal. 199 (2001) 224.
[33] J. Mijoin, G. Pérot, F. Bataille, J.L. Lemberton, M. Breysse, S. Kasztelan, Catal. Lett. 71 (2001) 139.
[34] M.V. Landau, D. Berger, M. Herskowitz, J. Catal. 159 (1996) 236.
[35] M. Daage, R.R. Chianelli, J. Catal. 149 (1994) 414.